Inorg. Chem. **2005**, *44*, 4637–4643

Geometrical and Electronic Structures of Dinuclear Complex Ions $\{(\mu\text{-bpym})[Cu(EAr_3)_2]_2\}^{2+}$ with Intramolecular "Organic Sandwich" Formation (E = P or As; Ar = Aryl; bpym = 2,2′-Bipyrimidine)†

Monika Sieger,‡ Conny Vogler,‡ Axel Klein,§ Axel Knödler,‡ Matthias Wanner,‡ Jan Fiedler,|| Stanislav Záliš,|| Theo L. Snoeck,⊥ and Wolfgang Kaim*,‡

Institut für Anorganische Chemie, Universität Stuttgart, Pfaffenwaldring 55, D-70550 Stuttgart, Germany, Institut für Anorganische Chemie, Universität zu Köln, Greinstrasse 6, D-50939 Köln, Germany, J. Heyrovský Institute of Physical Chemistry, Academy of Sciences of the Czech Republic, Dolejškova 3, CZ-18223 Prague, Czech Republic, and Van't Hoff Institute for Molecular Sciences, Universiteit van Amsterdam, Nieuwe Achtergracht 166, 1018 WV Amsterdam, The Netherlands

Received February 7, 2005

The compound $\{(\mu\text{-bpym})[Cu(AsPh_3)_2]_2\}(BF_4)_2$ (**1**) has been prepared and studied in comparison with the triphenylphosphine analogue **2**. Qualitatively, the structure of **1** with characteristically distorted copper(I) coordination caused by Ph/bpym/Ph sandwich interactions is similar to that of **2** and is approximately reproduced by DFT calculations for the model complex ions $\{(\mu\text{-bpym})[Cu(EMe_2Ph)_2]_2\}^{2+}$, E = P or As. In contrast, the dinuclear $\{(\mu\text{-bpym})[Cu(P(3\text{-Me-}C_6H_4)_3)_2]_2\}(BF_4)_2$ (**3**) displays a distinctly less distorted metal coordination geometry due to the steric requirements of the methyl groups in the *meta*-tolyl substituents. The electrochemical reduction of **1** is less reversible than for the phosphine analogues; the one-electron-reduced form $\mathbf{1}^{\bullet-}$ exhibits a broad, unresolved EPR signal at $g = 2.0023$. Resonance Raman spectroscopy of **1** shows the typical vibrations of the bpym ligand in agreement with the MLCT assignment of the long-wavelength transitions below 500 nm. All three dinuclear complexes exhibit luminescence at room temperature in the solid and in solution.

Copper(I) has been extensively used in the construction of elaborate and often fascinating supramolecular structures.[1] Its rather flexible coordination geometry and strong bonding to pyridine-type nitrogen donor atoms have contributed to this widespread application. For example, copper(I) complexes, including those with aromatic α-diimine ligands, have been widely studied with regard to luminescence.[2−6] Complexes of copper(I) with rigid 1,10-phenanthroline-type ligands exhibit strong emission from metal-to-ligand charge transfer (MLCT) or other excited states.[3] A recent report has shown that mixed α-diimine/organophosphine complexes of

* Author to whom correspondence should be addressed. E-mail: kaim@iac.uni-stuttgart.de.

† In memoriam to Dick Stufkens.

‡ Universität Stuttgart.
§ Universität zu Köln.
|| Heyrovsky Institute Prague.
⊥ Universiteit van Amsterdam.

(1) (a) Youinou, M.-T.; Rahmouni, N.; Fischer, J.; Osborn. J. A. *Angew. Chem.* **1992**, *104*, 771; *Angew. Chem., Int. Ed. Engl.* **1992**, *31*, 733. (b) Baxter, P. N. W.; Lehn, J.-M.; Kneisel, B. O.; Fenske, D. *Angew. Chem.* **1997**, *109*, 2067; *Angew. Chem., Int. Ed. Engl.* **1997**, *36*, 1978. (c) Baum, G.; Constable, E. C.; Fenske, D.; Housecroft, C. E.; Kulke, T.; Neuburger, M.; Zehnder, M. *J. Chem. Soc., Dalton Trans.* **2000**, 945. (d) Ruben, M.; Rojo, J.; Romero-Salguero, F. J.; Uppadine. L. H.; Lehn, J.-M. *Angew. Chem.* **2004**, *116*, 3705; *Angew. Chem., Int. Ed.* **2004**, *43*, 3644. (e) Perret-Aeba, L.-E.; von Zelewsky, A.; Dietrich-Buchecker, C.; Sauvage, J.-P. *Angew. Chem.* **2004**, *116*, 4582; *Angew. Chem., Int. Ed.* **2004**, *43*, 4482.

(2) (a) Dias, H. V. R.; Diyabalanage, H. V. K.; Rawashdeh-Omary, M. A.; Franzman, M. A.; Omary, M. A. *J. Am. Chem. Soc.* **2003**, *125*, 12072. (b) Omary, M A.; Rawashdeh-Omary, M. A.; Diyabalanage, H. V. K.; Dias, H. V. R. *Inorg. Chem.* **2003**, *42*, 8612.

(3) (a) Riesgo, E. C.; Hu, Y.-Z.; Bouvier, F.; Thummel, R. P.; Scaltrito, D. V.; Meyer, G. J. *Inorg. Chem.* **2001**, *40*, 3413. (b) Cuttell, D. G.; Kuang, S.-M.; Fanwick, P. E.; McMillin, D. R.; Walton, R. A. *J. Am. Chem. Soc.* **2002**, *124*, 6. (c) Williams, R. M.; De Cola, L.; Hartl, F.; Lagref, J.-J.; Planeix, J.-M.; De Cian, A.; Hosseini, M. W. *Coord. Chem. Rev.* **2002**, *230*, 253.

(4) (a) Che, M.-C.; Mao, Z.; Miskowski, V. M.; Tse, M.-C.; Chan, C.-K.; Cheung, K.-K.; Phillips, D. L.; Leung, K.-H. *Angew. Chem.* **2000**, *112*, 4250; *Angew. Chem., Int. Ed.* **2000**, *39*, 4084. (b) Vogler, A.; Kunkely, H. *Coord. Chem. Rev.* **2002**, *230*, 243.

(5) (a) Aconta, A.; Zink, J. I.; Cheon, J. *Inorg. Chem.* **2000**, *39*, 427. (b) Ranjan, S.; Dikshit, S. K. *Polyhedron* **1998**, *17*, 3071.

(6) Vogler, C.; Hausen, H.-D.; Kaim, W.; Kohlmann, S.; Kramer, H. E. A.; Rieker, J. *Angew. Chem.* **1989**, *101*, 1734; *Angew. Chem., Int. Ed. Engl.* **1989**, *28*, 1659.

10.1021/ic050207z CCC: $30.25
Published on Web 05/28/2005

copper(I) can exhibit strong emission from very long-lived excited states.[3b] In contrast to mono-, di-, or tetranuclear triorganophosphine complexes of copper(I)[3b,4] their triorganoarsine analogues have received much less attention;[5] a report on the luminescence of Cu(Tp)($AsPh_3$), Tp = hydrotris(pyrazolyl)borato, has been interpreted in terms of low-lying ligand-to-ligand charge-transfer excited states.[5a]

In this report we describe the characterization by structural, electrochemical, and spectroscopic methods of dinuclear molecule-bridged complexes {(μ-bpym)[Cu($AsPh_3$)$_2$]$_2$}(BF_4)$_2$ (**1**) and {(μ-bpym)[Cu(P(3-Me-C_6H_4)$_3$)$_2$]$_2$}(BF_4)$_2$ (**3**), bpym = 2,2′-bipyrimidine. The triphenylphosphine analogue of **1**, {(μ-bpym)[Cu(PPh_3)$_2$]$_2$}(BF_4)$_2$ (**2**), has been shown to exhibit strong luminescence in the solid state and in solution,[6] an unusually pronounced effect for dicopper(I) species connected through a conjugated π system. The crystal structure of **2** exhibits a remarkable "intramolecular organic sandwich" configuration where the central 2,2′-bipyrimidine acceptor ligand interacts in $\pi/\pi/\pi$ fashion with two phenyl rings from the coligands above and below the central plane.[6,7] This motif has been found later in other such complexes[8] and even in the radical species {(μ-bptz)[Cu(EPh_3)$_2$]$_2$}(BF_4), bptz = 3,6-bis(2-pyridyl)-1,2,4,5-tetrazine, E = P or As;[9] DFT calculations are employed here to investigate this effect as an intramolecular phenomenon.

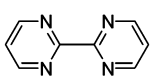

bpym

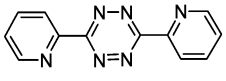

bptz

Experimental Section

Instrumentation. EPR spectra were recorded in the X band on a Bruker System ESP 300 equipped with a Bruker ER035M gaussmeter and a HP 5350B microwave counter. ^{1}H NMR spectra were taken on a Bruker AC 250 spectrometer. UV/vis absorption spectra were recorded on Shimadzu UV160 and Bruins Instruments Omega 10 spectrophotometers. A Perkin-Elmer fluorescence spectrometer LS-3B served to record emission spectra. Cyclic voltammetry was carried out in 0.1 M Bu_4NPF_6 solutions using a three-electrode configuration (glassy carbon working electrode, Pt counter electrode, Ag/AgCl reference) and a PAR 273 potentiostat and function generator. The ferrocene/ferrocenium couple served as internal reference. In situ EPR measurements were performed using a two-electrode capillary.[10] Resonance Raman spectra were obtained for KNO_3 pellets by excitation with several laser lines, 457.9, 488, and 514.5 nm (SP 2016 argon ion laser) or 605 nm (Rhodamine 6G dye laser line, pumped by the argon ion laser). The spectra were recorded by a Dilor XY spectrometer.

Syntheses. The compounds {(μ-bpym)[Cu($AsPh_3$)$_2$]$_2$}(BF_4)$_2$ (**1**) and {(μ-bpym)[Cu(P(3-Me-C_6H_4)$_3$)$_2$]$_2$}(BF_4)$_2$ were obtained according to a reported general procedure.[6,7] Yields of the yellow products after crystallization were 54% (**1**) and 60% (**3**).

Data for 1. ^{1}H NMR (acetone-d_6): 7.4 (m, 60H, Ph), 8.18 (t, 2H, H$^{5,5'}$ bpym), 9.48 (d, 4H, H$^{4,4',6,6'}$ bpym); J = 6.4 Hz. UV/vis (CH_2Cl_2): λ_{max} = 350, 480 sh nm. Cyclic voltammetry (DMF/0.1 M Bu_4NPF_6, 100 mV/s, 213 K): $E_{1/2}$ (ΔE_{pp}) = −1.27 V (130 mV), −1.83 V (120 mV). Anal. Calcd for $C_{80}H_{66}As_4B_2Cu_2F_8N_4$ (M_r = 1683.84): C, 57.06; H, 3.95; N, 3.33. Found: C, 56.74; H, 3.96; N, 3.32.

Data for 3. ^{1}H NMR (acetone-d_6): 2.78 (s, 36H, CH_3), 7.1 (m, 48H, tolyl-CH), 7.91 (t, 2H, H$^{5,5'}$ bpym), 9.23 (d, 4H, H$^{4,4',6,6'}$ bpym); J = 5.7 Hz. UV/vis ($CHCl_3$): λ_{max} = 368, 465 sh nm. Cyclic voltammetry (DMF/0.1 M Bu_4NPF_6, 100 mV/s, 218 K): $E_{1/2}$ (ΔE_{pp}) = −1.29 V (65 mV), −1.88 V (110 mV). Anal. Calcd for $C_{92}H_{90}B_2Cu_2F_8N_4P_4$ (M_r = 1676.35): C, 65.92; H, 5.41; N, 3.34. Found: C, 65.94; H, 5.31; N, 2.98.

Crystallography. Single crystals of **1**·2H_2O and **3** were obtained from saturated solutions in reagent grade methanol. Data were collected at 173 K using a Siemens P3 diffractometer (λ = 0.710 73 Å). The structures were solved using direct methods with refinement by full-matrix least-squares on F^2, employing the program package SHELXTL[11] and the program X-SHAPE[12] for absorption correction. All atoms other than hydrogen were refined anisotropically; hydrogen atoms were introduced using appropriate riding models.

DFT Calculations. Due to the size of the system, the phenyl groups on E without π interaction with μ-bpym were replaced by methyl groups. Ground-state electronic structure calculations on these model complexes have been done by the density-functional theory (DFT) method using the Gaussian 03[13] and ADF2004.1[14] program packages. The lowest excited states of the closed-shell complexes were calculated by the time-dependent DFT (TD-DFT) method (G03); the solvent influence was modeled by the conductor-like polarizable continuum model (CPCM).[15]

Within the Gaussian-03 program 6-31g* polarized double-ζ basis sets[16] were used in connection with Becke's hybrid three parameter functional with the Lee, Yang, and Parr correlation

(7) Vogler, C.; Kaim, W.; Hausen, H.-D. *Z. Naturforsch.* **1993**, *48b*, 1470.
(8) Schwach, M.; Hausen, H.-D.; Kaim, W. *Chem. Eur. J.* **1996**, *2*, 446.
(9) (a) Schwach, M.; Hausen, H.-D.; Kaim, W. *Inorg. Chem.* **1999**, *38*, 2242. (b). Ye, S.; Kaim, W.; Sarkar, B.; Schwederski, B.; Lissner, F.; Schleid, T.; Duboc-Toia, C.; J. Fiedler, J. *Inorg. Chem. Commun.* **2003**, *6*, 1196.
(10) Kaim, W.; Ernst, S.; Kasack, V. *J. Am. Chem. Soc.* **1990**, *112*, 173.
(11) (a) Sheldrick, G. M. *SHELXTL*; Bruker Analytical X-ray Systems: Madison, WI, 1998. (b) Sheldrick, G. M. *SHELXL-97: A Program for Crystal Structure Determination*; Universität Göttingen: Göttingen, Germany, 1997.
(12) (a) *Program X-Shape*, version 1.06; Stoe & Cie GmbH: Darmstadt, Germany, 1999. (b) Herrendorf, W. *Program Habitus*; Ph.D. Thesis, Universitaet Karlsruhe, Germany, 1993.
(13) Frisch, M. J.; Trucks, G. W.; Schlegel, H. B.; Scuseria, G. E.; Robb, M. A.; Cheeseman, J. R.; Montgomery, J. A., Jr.; Vreven, T.; Kudin, K. N.; Burant, J. C.; Millam, J. M.; Iyengar, S. S.; Tomasi, J.; Barone, V.; Mennucci, B.; Cossi, M.; Scalmani, G.; Rega, N.; Petersson, G. A.; Nakatsuji, H.; Hada, M.; Ehara, M.; Toyota, K.; Fukuda, R.; Hasegawa, J.; Ishida, M.; Nakajima, T.; Honda, Y.; Kitao, O.; Nakai, H.; Klene, M.; Li, X.; Knox, J. E.; Hratchian, H. P.; Cross, J. B.; Adamo, C.; Jaramillo, J.; Gomperts, R.; Stratmann, R. E.; Yazyev, O.; Austin, A. J.; Cammi, R.; Pomelli, C.; Ochterski, J. W.; Ayala, P. Y.; Morokuma, K.; Voth, G. A.; Salvador, P.; Dannenberg, J. J.; Zakrzewski, V. G.; Dapprich, S.; Daniels, A. D.; Strain, M. C.; Farkas, O.; Malick, D. K.; Rabuck, A. D.; Raghavachari, K.; Foresman, J. B.; Ortiz, J. V.; Cui, Q.; Baboul, A. G.; Clifford, S.; Cioslowski, J.; Stefanov, B. B.; Liu, G.; Liashenko, A.; Piskorz, P.; Komaromi, I.; Martin, R. L.; Fox, D. J.; Keith, T.; Al-Laham, M. A.; Peng, C. Y.; Nanayakkara, A.; Challacombe, M.; Gill, P. M. W.; Johnson, B.; Chen, W.; Wong, M. W.; Gonzalez, C.; Pople, J. A. *Gaussian 03*, revision B.2; Gaussian, Inc.: Pittsburgh, PA, 2003.
(14) (a) Fonseca Guerra, C.; Snijders, J. G.; te Velde, G.; Baerends, E. J. *Theor. Chim. Acc.* **1998**, *99*, 391. (b) te Velde, G.; Bickelhaupt, F. M.; van Gisbergen, S. J. A.; Fonseca Guerra, C.; Baerends, E. J.; Snijders, J. G.; Ziegler, T. *J. Comput. Chem.* **2001**, *22*, 931.
(15) Cossi, M.; Rega, N.; Scalmani, G.; Barone, V. *J. Comput. Chem.* **2003**, *24*, 669.
(16) (a) Hariharan, P. C.; Pople, J. A. *Theor. Chim. Acta* **1973**, *28*, 213. (b) Rassolov, V. A.; Pople, J. A.; Ratner, M. A.; Windus, T. L. *J. Chem. Phys.* **1998**, *109*, 1223.

Table 1. Crystallographic and Structure Refinement Data for $\mathbf{1}\cdot 2H_2O$ and **3**

param	**1**	**3**
formula	$C_{80}H_{70}As_4B_2Cu_2F_8N_4O_2$	$C_{92}H_{90}B_2Cu_2F_8N_4P_4$
MW	1715.75	1676.26
cryst system	triclinic	monoclinic
space group	$P\bar{1}$	*C*2/*c*
a (Å)	11.875(2)	34.1607(4)
b (Å)	12.704(3)	12.11610(10)
c (Å)	14.941(3)	21.5496(3)
α (deg)	64.90(3)	90.00
b (deg)	71.89(3)	107.859(10)
g (deg)	74.60(3)	90.00
V (Å^3)	1916.5(7)	8489.48(17)
Z	1	4
ρ_{calc} (g cm^{-3})	1.487	1.312
F(000)	862	3480
limiting indices	$-1 < h < 16$, $-17 < k < 17$, $-19 < l < 21$	$-44 < h < 44$, $15 < k < 14$, $-27 < l < 26$
reflcns collcd/ unique/R_{int}	10 888/10 397/0.0359	72 526/9603/0.0596
data/restr/params	10 397/3/469	9603/0/507
GOOF on F^2	1.036	1.068
final R1, wR2 [$I > 2\sigma(I)$]	0.0525, 0.1090	0.0601, 0.1525
R_1, wR_2 (all data)	0.0905, 0.1272	0.0763, 0.1638
largest diff peak and hole (e·Å^{-3})	0.752 and −0.618	0.690 and −0.488

Table 2. Selected Bond Lengths (Å) and Angles (deg) of $\mathbf{1}\cdot 2H_2O$[a]

Cu−N1	2.066(4)	As2−C41	1.935(5)
Cu−N2′	2.105(4)	As2−C51	1.953(4)
Cu−As1	2.314(1)	As2−C61	1.940(5)
Cu−As2	2.391(1)	C1−C1′	1.482(8)
As1−C11	1.947(4)	N1−C1	1.339(5)
As1−C21	1.940(4)	C1−N2	1.339(5)
As1−C31	1.953(4)		
N1−Cu−N2′	80.54(14)	C31−As1−Cu	109.6(1)
N1−Cu−As1	126.45(10)	C41−As2−Cu	118.8(1)
N2′−Cu−As1	120.43(10)	C51−As2−Cu	103.6(1)
N1−Cu−As2	100.15(10)	C61−As2−Cu	120.2(1)
N2′−Cu−As2	98.79(10)	C1′−N2′−Cu	111.9(3)
As1−Cu−As2	121.08(4)	C1−N1−Cu	113.1(3)
C11−As1−Cu	116.1(1)	N1−C1−C1′	117.0(4)
C21−As1−Cu	120.6(1)	N2−C1−C1′	117.0(4)

[a] Symmetry transformation used to generate equivalent atoms: (prime) $-x, -y, -z + 2$.

functional (B3LYP)[17] (G03/B3LYP). Within the ADF program Slater-type orbital (STO) basis sets of triple-ζ quality with polarization functions were employed. The inner shells were represented by frozen core approximation (1s for C, N, 1s−2p for P, 1s−3p for As, and 1s−2p for Cu were kept frozen). The following density functionals were used within ADF: the local density approximation (LDA) with VWN parametrization of electron gas data or the functional including Becke's gradient correction[18] to the local exchange expression in conjunction with Perdew's gradient correction[19] to the LDA expression (ADF/BP).

The geometries of all complexes were optimized without any symmetry constraints; the orientation with the bpym ligand located in the *xy* plane and the Cu atoms on the *x* axis is used for the discussion.

(17) Stephens, P. J.; Devlin, F. J.; Cabalowski, C. F.; Frisch, M. J. *J. Phys. Chem.* **1994**, *98*, 11623
(18) (a) Becke, A. D. *Phys. Rev. A* **1988**, *38*, 3098. (b) Becke, A. D. *Phys. Rev. A* **1988**, *38*, 3098.
(19) Perdew, J. P. *Phys. Rev. A* **1986**, *33*, 8822.

Table 3. Selected Bond Distances (Å) and Angles (deg) of **3**

Cu−N2	2.118(2)	N1−C1	1.334(3)
Cu−N1	2.128(2)	N2−C2	1.340(3)
Cu−P1	2.244(1)	C1−C2	1.469(5)
Cu−P2	2.278(1)		
N2−Cu−N1	78.62(9)	C42−P2−Cu	119.1(1)
N2−Cu−P1	114.35(7)	C14−P1−Cu	117.9(1)
N1−Cu−P1	124.93(7)	C7−P1−Cu	115.0(1)
N2−Cu−P2	106.97(7)	C21−P1−Cu	111.1(1)
N1−Cu−P2	100.71(7)	C1−N1−Cu	113.3(2)
P1−Cu−P2	122.34(3)	C2−N2−Cu	113.3(2)
C35−P2−Cu	117.3(1)	N1−C1−C2	116.7(2)
C28−P2−Cu	104.9(1)	N2−C2−C1	117.0(2)

Results and Discussion

Structures and DFT Calculations. The molecular structures of the two new dinuclear compounds **1** and **3** exhibit bridging[6−8] of two copper(I) centers by the symmetrically bis-chelating bpym ligand in the complex dication. Crystal data are listed in Table 1, and selected bond parameters are summarized in Tables 2 and 3. Figures 1 and 2 show

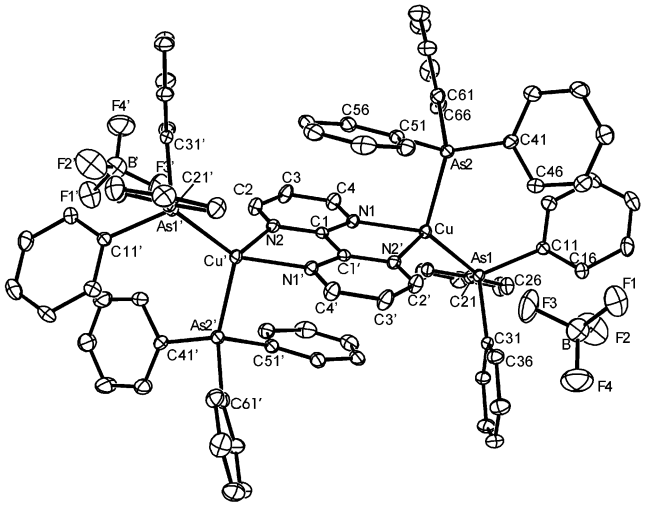

Figure 1. Molecular structure of the dication and BF_4^- ions in the crystal of $\mathbf{1}\cdot 2H_2O$.

representations of the molecular structures of the dications in the crystal.

The bridging ligand bpym induces metal−metal distances of very similar magnitude, viz., 5.561 Å for **1**, 5.622 Å for

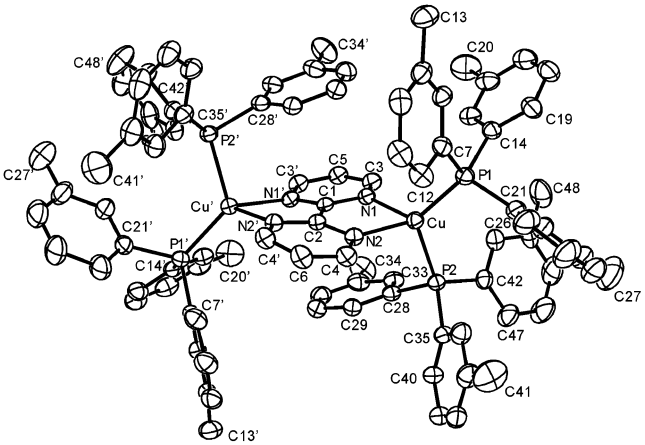

Figure 2. Molecular structure of the dication in the crystal of **3**.

Table 4. Structural Characteristics of Complexes **1**−**3**

	1	**2**[a]	**3**
		Distances (Å)	
Cu−Cu	5.561	5.622	5.656
Cu−E1[b]	2.314(1)	2.231(1)	2.244(1)
Cu−E2[b]	2.391(1)	2.295(1)	2.278(1)
Δd[c]	0.077	0.064	0.034
Cu−N1	2.066(4)	2.087(2)	2.118(2)
Cu−N2	2.105(4)	2.119(2)	2.128(2)
d_{nb}[d]	3.46	3.15	3.23 and 3.36
X−Y[d]	C1−C56	C1−C56	N1−C28 and C4−C33/C1−C29
		Angles (deg)	
Cu−E2−Cx[b,e]	103.6(1)	104.7(1)	104.9(1)
ω_1[f]	138.9	139.4	129.0
ω_2[f]	99.7	98.0	107.8
$\Delta\omega$[f]	39.2	41.4	21.2
θ[g]	11.8	14.0	14.5
Σ[h]	647.4	646.7	647.9

[a] From ref 7. [b] E = As (**1**) or P (**2**, **3**). [c] $\Delta d = d_{Cu-E2} - d_{Cu-E1}$. [d] d_{nb}: closest nonbonding distance between atom X of bpym and atom Y of a Ph ring. [e] Cx: *ipso* C atom of phenyl ring involved in $\pi/\pi/\pi$ interaction: C51 for **1** and **2**; C28 for **3**. [f] ω: angles between Cu(bpym)Cu plane and Cu−E bonds; $\Delta\omega = \omega 1 - \omega 2$. [g] Dihedral angle between bpym and interacting aryl rings. [h] Sum of angles on Cu.

2, and 5.656 Å for **3**. The slight lengthening in that series results from a lengthening of the Cu−N bonds from 2.086 Å for **1** to 2.122 Å for **3** (averages). The geometry within the bpym bridge shows little variation, including the inter-ring distances of 1.47 ± 0.01 Å which reflect a rather modest degree of metal-to-ligand π back-donation.[20] However, Figures 1 and 2 illustrate that there is a significant difference in the intramolecular arrangement of the dications in **1** and **3**: the triphenylarsine complex **1** crystallizes isostructurally with the triphenylphosphine analogue **2**[6,7] and exhibits a rather similar molecular arrangement with a $\pi/\pi/\pi$ sandwich formation involving the planar bpym as central π acceptor and two phenyl rings from $AsPh_3$ coligands as donors above and below (Figure 1). Although not quite a classical stacking[3a,21] due to dihedral angles of about $\theta = 12°$ between the Ph and bpym planes (Table 4), some atoms of the different rings come rather close, e.g. at 3.46 Å for C1−C56 in **1**, documenting the $\pi/\pi/\pi$ attraction. The shortest such nonbonding distance in **2** was determined at 3.15 Å,[6,7] this much smaller value being a consequence of shorter Cu−E and E−C bonds for E = P relative to E = As.[22] Methyl substitution in the *meta* positions of the phenyl rings causes a significant change for **3**, presumably due to steric interference: The shortest nonbonding distances between the aryl and bpym rings are increased to 3.23 Å (N1−C28) and 3.36 Å for C1−C29 and C4−C33 (Table 4).

As a consequence of the $\pi/\pi/\pi$ interaction in complexes **1**−**3**, the bonding to the two EPh_3 ligands at each copper atom is significantly different: the $E(aryl)_3$ ligand of which one aryl group interacts with bpym adopts an "axial" position

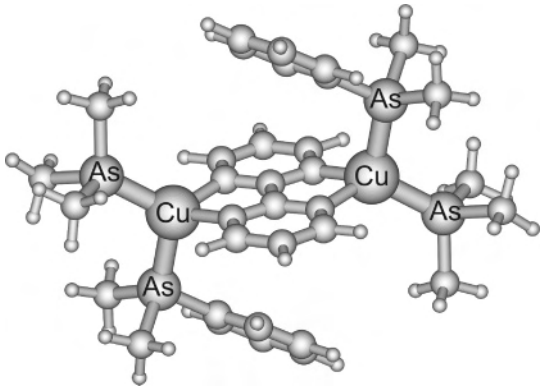

Figure 3. DFT (G03/B3LYP) optimized geometry of $\{(\mu\text{-bpym})[Cu(AsPhMe_2)(AsMe_3)]_2\}^{2+}$.

with elongated Cu−E bonds in a coordination geometry approaching the trigonal pyramid. Characteristic parameters for this interaction are summarized in Table 4.

Taking into account the ca. 0.1 Å longer bonds to As relative to P[22] the elongation parameter $\Delta d = d_{Cu-E(2)} - d_{Cu-E(1)}$ decreases from 0.077 Å for **1** and 0.064 Å for **2** to 0.034 Å for **3**. The angles also illustrate the distortion induced by the $\pi/\pi/\pi$ interaction: the Cu−As2−C51 angle of 103.6(1)° is much reduced in comparison to the other Cu−As−C angles, ranging between 116 and 121°. For **2** the corresponding Cu−P2−C51 angle is 104.7(1)°, and in **3** the Cu−P2−C28 angle is 104.9(1)°. Another parameter is the angle ω between the Cu−E bond and the central coordination plane including the metal atoms and the bridging ligand. These values show a difference of $\Delta\omega$ = 39.2° between $\omega 1$ = 138.9° (E = As1) and $\omega 2$ = 99.7° (E = As2) for compound **1**; for the analogous **2** the corresponding values were similar at 139.4 and 98.0° ($\Delta\omega$ = 41.4°).[7] For **3**, on the other hand, the difference is about halved to only $\Delta\omega$ = 21.2° (Table 4).

Thus, the distortion due to the $\pi/\pi/\pi$ interaction in **1** takes place despite the longer Cu−As vs Cu−P bonds whereas a relatively minor perturbation such as the introduction of methyl substituents in the *meta* positions at each phenyl ring causes considerable diminishing of this interaction.

DFT calculations were therefore employed to investigate the experimentally observed intramolecular effects for a model system $\{(\mu\text{-bpym})[Cu(EPhMe_2)(EMe_3)]_2\}^{2+}$, where only the two phenyl groups engaging in π/π interaction were retained (Figure 3).

The DFT-optimized structure of $\{(\mu\text{-bpym})[Cu(AsPhMe_2)(AsMe_3)]_2\}^{2+}$ depicted in Figure 3 indicates the distortion caused by $\pi/\pi/\pi$ interaction. Calculated bond lengths and angles shown in Table 5 qualitatively reproduce the essential features of the experimental structures of **1** and **2**, with significant dependence on the basis sets used. In agreement with experiment there is a lengthening of the Cu−N bonds on going from **1** to **2**. The calculated distortions as illustrated by N−Cu−E and E−Cu−E angles are smaller than the experimental ones because of the substitution of most phenyl rings by methyl. As a consequence, the final geometry arrangement is determined by an interplay of electronic (π/π attraction)[21] and steric repulsion effects.

(20) Baumann, F.; Stange, A.;. Kaim, W. *Inorg. Chem. Commun.* **1998**, *1*, 305.
(21) (a) Janiak, C. *J. Chem. Soc., Dalton Trans.* **2000**, 3885. (b) Lu, W.; Chan, M. C. W.; Cheung, K.-K.; Che, C.-M. *Organometallics* **2001**, *20*, 2477.
(22) Otto, S.; Muller, A. J. *Acta Crystallogr.* **2001**, *C57*, 1405.

Table 5. Selected DFT Calculated Bond Lengths (Å) and Angles (deg) for Model Complexes $\{(\mu\text{-bpym})[Cu(EPhMe_2)(EMe_3)]_2\}^{2+}$

	E = As			E = P		
	G03/B3LYP	ADF/BP	expt[a]	G03/B3LYP	ADF/BP	expt[b]
Cu−N1	2.047	2.096	2.066	2.062	2.169	2.118
Cu−N2′	2.049	2.109	2.105	2.069	2.174	2.128
Cu−E1	2.298	2.372	2.314	2.250	2.295	2.244
Cu−E2	2.318	2.398	2.391	2.254	2.312	2.278
N1−C1	1.345	1.349	1.339	1.347	1.350	1.334
C1−C1′	1.466	1.464	1.482	1.463	1.471	1.469
N1−Cu−N2′	82.0	79.7	80.54	80.9	77.1	78.62
N1−Cu−E1	125.1	124.4	126.45	117.4	116.0	124.93
N2′−Cu−E1	120.1	118.9	120.43	113.2	113.5	114.35
N1−Cu−E2	107.8	107.3	100.15	113.0	112.5	106.97
N2′−Cu−E2	105.2	105.1	98.79	110.0	109.9	100.71
E1−Cu−E2	114.6	116.4	121.08	116.6	120.1	122.34
C1′−N2′−Cu	111.6[c]	112.4[c]	112.5[c]	112.6[c]	114.0[c]	113.3[c]
N1−C1−C1′	117.0[c]	117.1[c]	117.0[c]	116.9[c]	117.2[c]	116.9[c]

[a] Experimental values for $\mathbf{1}\cdot 2H_2O$. [b] Experimental values for **2**, from ref 7. [c] Average value.

Electrochemistry and EPR Spectroscopy. In contrast to the triarylphosphine analogues **2**[6,7] and **3**, the triphenylarsine compound **1** undergoes only irreversible reduction at room temperature. The lability of As−C bonds on electron addition despite the enhanced electron affinity[23] relative to corresponding phosphines is responsible for this previously noted[9] effect. At low temperatures (213 K) in DMF solution two quasi-reversible reduction waves can be observed at potentials which suggest[6,7] the successive reduction of the 2,2′-bipyrimidine bridge in **1**. The potentials at −1.27 and −1.83 V and their difference of 0.56 V are similar to those of **2** ($E_1 = -1.23$ V, $E_2 = -1.86$ V, $\Delta E = 0.63$ V) or **3** ($E_1 = -1.29$ V, $E_2 = -1.88$ V, $\Delta E = 0.59$ V).

Low temperature (<275 K) intra muros reduction of **1** in an EPR spectrometer yielded a broad, unresolved EPR signal of the radical complex $\{(\mu\text{-bpym})[Cu(AsPh_3)_2]_2\}^{\bullet+}$ at $g = 2.0023$. A similar g value close to the free electron value has been reported for the related $\{(\mu\text{-bptz})[Cu(AsPh_3)_2]_2\}^{\bullet+}$ at $g = 2.0053$ (bptz = 3,6-bis(2-pyridyl)-1,2,4,5-tetrazine).[9b] The replacement of ^{31}P ($I = 1/2$) by ^{75}As ($I = 3/2$, 100% natural abundance) causes an increase in the total number of theoretical lines to 12 285, even without considering the nonequivalence of ^{63}Cu and ^{65}Cu isotopes;[24] this large number readily explains the lack of resolution of the hyperfine structure. However, from the total spectral width of 15 mT and the assumption of ^{1}H, ^{14}N, and $^{63,65}Cu$ hyperfine coupling as in the triphenylphosphine analogue[6,7] one can estimate[25] a hyperfine coupling of about 0.68 mT for four ^{75}As nuclei. This value compares with an almost identical ^{31}P coupling of 0.69 mT for reduced **2**,[6,7] reflecting the relatively similar isotropic hyperfine coupling constants of 474.79 mT (^{31}P) and 523.11 mT for ^{75}As.[26]

Absorption, Emission, and Resonance Raman Spectroscopy. Dinuclear complexes of 2,2′-bipyrimidine with electron-rich metal atoms exhibit several low-energy metal-to-ligand charge transfer (MLCT) transitions due to the presence of three low-lying unoccupied π^* orbitals in bpym.[27] Assignments of these transitions can be facilitated via resonance Raman spectroscopy[27a] or high-resolution EPR of one-electron reduced forms;[27b] however, the d orbital splitting is different in a d^{10} case (Cu^{I})[28] compared to complexes of low-spin d^6 centers (e.g. Mo^0, W^0)[27a] or of d^8 systems (e.g. Pt^{II}).[29] The compounds **1**−**3** exhibit comparable absorption spectra in solution with maxima around 360 nm and broad long-wavelength shoulders at about 460 nm (Figure 4, Table 6). The solvatochromism of these bands[27c,d] is rather small in the available solvents (Table 6). The spectral appearance suggests the presence of at least three absorption bands in the visible and near UV regions.

Resonance Raman spectroscopy of **1** in KNO_3 shows enhanced vibrations at 1565 (m), 1521 (w), 1462 (vs), 1359 (w), and 1027 (w) cm^{-1} upon excitation with 457.9 nm light. These values, typical for bpym framework vibrations,[27a] have similarly been obtained for dinuclear complexes $(\mu\text{-bpym})[M(CO)_4]_2$, M = Mo and W,[27a] at about 1556, 1470, 1332, and 1033 cm^{-1}, and for $(\mu\text{-bpym})[PtCl_2]_2$ at 1557 and 1507 cm^{-1}.[29] When irradiated with longer wavelength at 488 and 514.5 nm the bands lose intensity, and the two main bands at 1565 and 1462 cm^{-1} change in relative intensity which points to several close-lying electronic transitions of slightly different character forming the broad long-wavelength band. Another noteworthy observation is the appearance of a band at 1359 cm^{-1} which is attributed to the inter-ring vibration ν(C−C). This band should be enhanced only when the LUMO is the target orbital and if there is already an appreciable amount of electron density at the ring-connecting atoms in the ground state.[29] From the intensity variations observed for this inter-ring stretching band among the

(23) Giordan, J. C.; Moore, J. H.; Tossell, J. A.; Kaim, W. *J. Am. Chem. Soc.* **1985**, *107*, 5600.
(24) Kaim, W.; Moscherosch, M. *J. Chem. Soc., Faraday Trans.* **1991**, *87*, 3185.
(25) Calculated according to $a(^{75}As) = [15\text{ mT} - 8a(^{14}N) - 2a(^{1}H) - 6a(^{63,65}Cu)]/12$.
(26) Weil, J. A.; Bolton, J. R.; Wertz, J. E. *Electron Paramagnetic Resonance*; Wiley: New York, 1994.
(27) (a) Kaim, W.; Kohlmann, S.; Lees, A. J.; Snoeck, T. L.; Stufkens, D. J.; Zulu, M. M. *Inorg. Chim. Acta* **1993**, *210*, 159. (b) Kaim, W. *Inorg. Chem.* **1984**, *23*, 3365. (c) Dodsworth, E. S.; Lever, A. B. P. *Coord. Chem. Rev.* **1990**, *97*, 271. (d) Kaim, W.; Kohlmann, S. *Inorg. Chem.* **1986**, *25*, 3306.
(28) Vogler, C.; Kaim, W. *Z. Naturforsch.* **1992**, *47b*, 1057.
(29) Kaim, W.; Dogan, A.; Wanner, M.; Klein, A.; Tiritiris, I.; Schleid, T.; Stufkens, D. J.; Snoeck, T. L.; McInnes, E. J. L.; Fiedler, J.; Zalis, S. *Inorg. Chem.* **2002**, *41*, 4139.
(30) Moore; K. J.; Petersen, J. D. *Polyhedron* **1983**, *2*, 279. (b) Overton, C.; Connor, J. A. *Polyhedron* **1982**, *1*, 53.

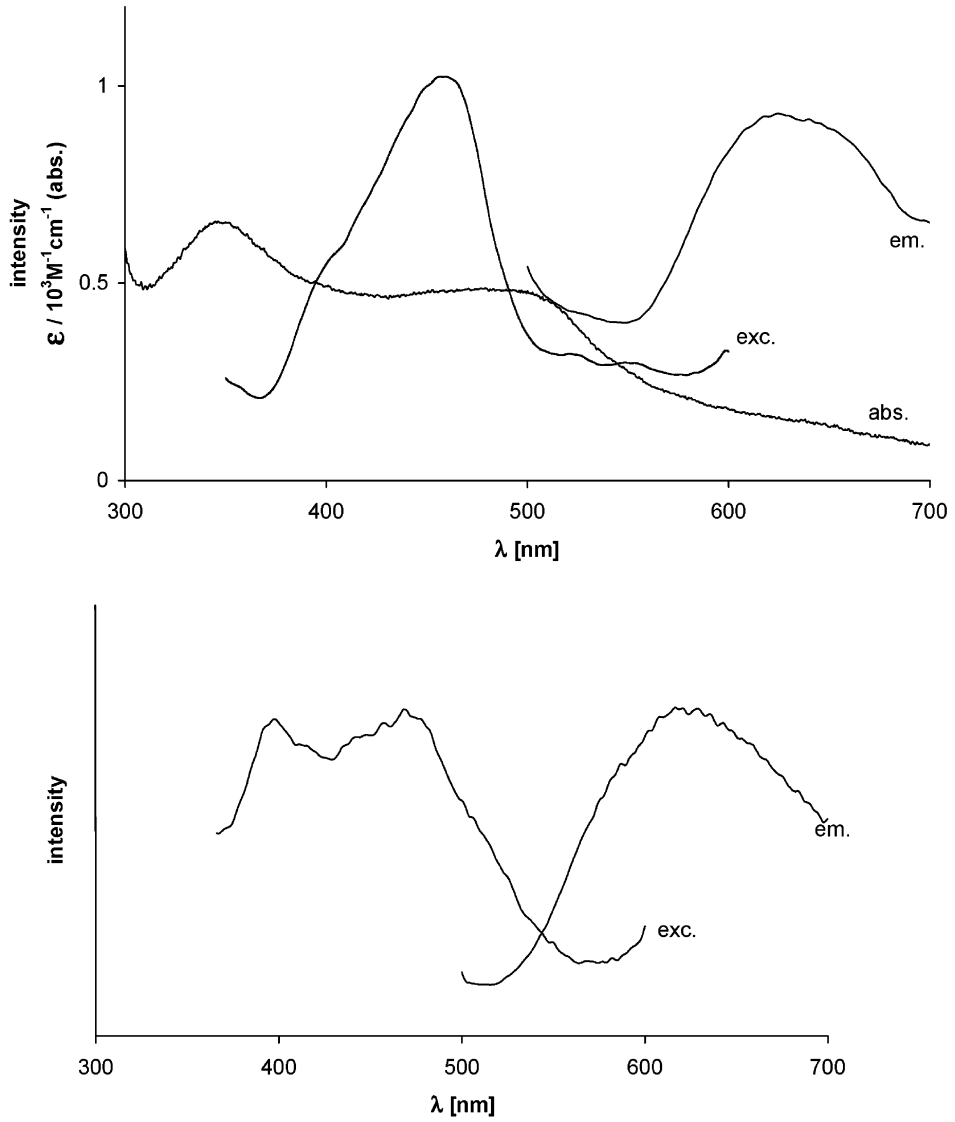

Figure 4. Absorption, emission (λ_{ex} = 470 nm), and excitation spectra (λ_{em} = 630 nm) of **1** in CH_2Cl_2 (top) and emission (λ_{ex} = 470 nm) and excitation spectra (λ_{em} = 630 nm) of **1** in the solid (bottom).

mentioned bpym complexes one can conclude that the copper(I) centers (d^{10}) in **1** represent stronger π donors toward the π accepting bridge than the Cl_2Pt group (d^8) in (μ-bpym)$[PtCl_2]_2$[29] but weaker donors than the $M(CO)_4$ (M = W or Mo) complex fragments (d^6) in (μ-bpym)-$[M(CO)_4]_2$.[27]

All three complexes **1**−**3** are luminescent in the solid state and in dichloromethane or chloroform[6] solutions; the emission is weakest for **3**. Emission and excitation spectra of **1** in CH_2Cl_2 solution and in the solid are shown in Figure 4; Table 6 summarizes the data.

The excitation spectra for **1** and **3** confirm the presence of two absorption features at about 460 and 400 nm, in addition to the more intense band at around 360 nm.

Figure 5 illustrates the TD DFT based assignment of the lowest allowed excitations for the chosen model for **1**.

Figure 5 shows that the set of highest occupied orbitals is formed by pairs of molecular orbitals with contributing symmetric (s) or antisymmetric (a) combinations of Cu 3d orbitals. Both the HOMO and HOMO-1 are mainly composed of Cu d_{xz} orbitals with large contributions from the As ligands; lower lying occupied orbitals have prevailing Cu 3d character. The LUMO is formed from the b_{2u} unoccupied orbital of the bpym ligand interacting with the antisymmetric combination of Cu d_{xz} orbitals. The second

Table 6. Absorption and Emission Wavelengths[a] of Complexes **1**−**3**

	1	**2**	**3**[b]
λ_{abs}	348[c,d]	357	368[e]
	480 br	438 sh	465 sh
λ_{em} (λ_{exc})			
solution	625 (470)	758 (436)	540 (465)
solid	630 (470)	630 (426)	620 (460)
λ_{ex} (λ_{em})			
solution	460 (630)	n.r.	460 (540)
	400 sh (630)		400 sh (540)
solid	470 (630)	n.r.	467 (620)
	398 (630)		398 (620)

[a] Wavelengths λ in nm; solvent CH_2Cl_2 for **1** and **3** and $CHCl_3$ for **2**. [b] From ref 6. [c] ϵ = 6300 M^{-1} cm^{-1}. [d] 345 nm in acetone, 351 nm in DMF. [e] 352 nm in acetone, 372 nm in DMF.

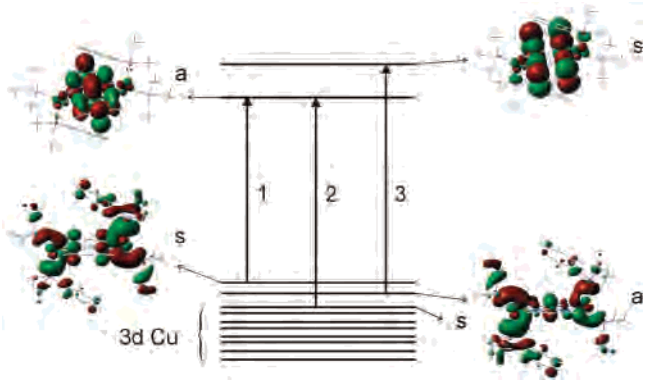

Figure 5. Representations of orbitals involved in the lowest allowed TD DFT calculated transitions for $\{(\mu\text{-bpym})[Cu(AsPhMe_2)(AsMe_3)]_2\}^{2+}$. Symbols "s" and "a" indicate the symmetric or antisymmetric combination of Cu orbitals, respectively.

lowest unoccupied molecular orbital (SLUMO, LUMO+1) is formed from b_{1g} (bpym) and the symmetric combination of Cu d_{xz} orbitals. TD DFT calculations on the model complex underestimate the lowest transition energies. In agreement with previous results on carbonylmetal complexes of bpym[27,30] the lowest energy absorption is characterized as a transition from the HOMO to the bpym-based LUMO (calculated at 581 nm, oscillator strength 0.146), a metal-to-ligand charge transfer together with ligand-to-ligand charge transfer (MLCT/LLCT). A second, weaker transition is identified as the HOMO-2−LUMO transition (calculated at 550 nm, oscillator strength 0.019), whereas the third band is attributed to the excitation from HOMO-1 into the SLUMO (calculated at 420 nm, oscillator strength 0.159).

While the emission wavelengths for the solids remain rather constant at about 620 nm, there are variations of the emission maxima in solution. In contrast to **2** for which the emission maximum in fluid solution showed a marked red-shift compared to the solid-state emission,[6] those values are almost the same for **1** under both conditions while **3** shows even a high-energy shift. Assuming that the emitting states of the complexes have the same ^{3}MLCT character in the solid (in fact, **1** and **2** crystallize isostructurally), the differences in fluid solution are tentatively attributed to different degrees of retained $\pi/\pi/\pi$ interaction, decreasing in the order **2** > **1** > **3**.

Summarizing, we have shown experimentally that the $\pi/\pi/\pi$ "organic sandwich" formation in the complexes $\{(\mu\text{-bpym})[Cu(EAr_3)_2]_2\}^{2+}$ is a sensitive kind of intramolecular interaction, easily perturbed by steric effects. However, it occurs for both E = P and E = As and is a molecular phenomenon, reproducible by DFT calculations for a model system. Different degrees of intramolecular $\pi/\pi/\pi$ association may be partially responsible for the differences observed in emission properties. On the other hand, the influence of increased spin−orbit coupling on going from E = P to E = As appears to be small as confirmed also by EPR spectroscopy of the one-electron reduced forms. The observation of "organic sandwiches" with other bridging ligands, including radicals,[9] suggests that such structural motifs may be constructed also in other settings which would allow a further study of the correlation with physical properties.

Acknowledgment. This work has been supported by the Deutsche Forschungsgemeinschaft, the Fonds der Chemischen Industrie, and the European Union (COST D14 Action). S.Z. also thanks the Grant Agency of the Academy of Sciences of the Czech Republic (Grant 1ET400400413). We also thank Dr. W. Schwarz for crystallographic data collection.

Supporting Information Available: X-ray crystallographic files in CIF format for **1**·2H_2O and **3**. This material is available free of charge via the Internet at http://pubs.acs.org.

IC050207Z